MICROSTRUCTURAL EVOLUTION OF A DP800 STEEL COMPOSITION UNDER DIFFERENT CASTING TECHNOLOGIES

[1]Ajitesh SHARMA, [1]Carl SLATER, [1]Claire DAVIS

[1]WMG, University of Warwick, Coventry, United Kingdom, ajitesh.sharma@warwick.ac.uk

https://doi.org/10.37904/metal.2025.5071

Abstract

Next generation casting technologies such as thin slab, belt or strip casting have gained popularity due to the reported energy saving, which can be as high as 1.6GJ/tonne when compared to conventional thick slab casting. However, these casting approaches result in changes in cooling rate during solidification and in thickness reduction to the required product geometry, which could affect the resulting microstructure and elemental segregation. In this work the secondary dendrite arm spacing (SDAS) and micro-segregation levels for the range of cooling rates relevant for different casting technologies (0.8 to 6°C/s) have been assessed using predicted COMSOL modelling coupled with known empirical SDAS and cooling rate relationships. A dual phase DP800 steel has been selected as the material to evaluate its specific role in micro-segregation. SEM-EDX grid maps have been used to characterise micro-segregation levels. To complement the experimental observations, Thermo-Calc simulations were conducted to predict micro-segregation behaviour using both initial cooling rates and post-solidification profiles for validation. The segregation ratios have been mapped for various cooling rates, correlating to the casting relevant techniques enabling quantification of segregation severity. The influence of CR on the SDAS and microsegregation of Mn has been investigated in this study. The SDAS results show for a DP wedge mould, that at lower CR (~0.68℃/s) the dendritic structure is coarse with SDAS at 104.01µm (± 4.49µm), where the SDAS was refined at higher CR (~5.8℃/s) measured at 40.02µm (± 1.87µm). The SR behaviour showed a difference at the lower CR ~0.68℃/s and higher CR ~5.8℃/s as well as the mid-section (all of which can be broken down into three distinct regions) and will be discussed.

Keywords: Cooling rate, microsegregation, secondary dendrite arm spacing, solidification, casting

1. INTRODUCTION

Conventional continuous casting (CCC) is widely used in the production of steel grades in semi-finished shapes. Various cross-sectional products (such as billets, blooms or slabs) are produced, with slabs that include thick slab, thin slab and also strip casting. Thicknesses are typically in the range of 200-300mm for thick slabs, 50-100mm for thin slabs and 1-5mm for strip casts [1]. The cooling rate (CR) during solidification is primarily controlled by the size of the mould, where higher cooling rates are seen for thinner slabs. The CR is an important parameter affecting the solidification process with a direct influence on the secondary dendrite arm spacing (SDAS) and the extent of alloying element microsegregation in steel. The different casting technologies relating to the cast product sizes result in different CR, where CCC has a slow CR of 0.13℃/s at the centre of the slab compared to that of horizontal single belt casting (HSBC) which is much higher at 50℃/s [2, 3]. Thin slab casting (TSC) and strip casting have been reported to give CR of 45℃/s and 723℃/s respectively [4, 5].

The variation in cooling rates affect the morphology and SDAS, which in turn influence casting defects such as hot tearing, cracking and microsegregation [6]. The segregation of certain elements such as Mn into the interdendritic regions during solidification is inevitable in steels (especially DP steels) and can lead to

differences in hardness and strength, impacting the mechanical properties. Reported studies have shown that with increased cooling rates (0.05℃/s to 1.89℃/s, with the SDAS decreasing from 96.7μm to 47.4μm), causing segregation deviation parameter for Mn, a quantitative measure of microsegregation to increase significantly from approximately 0.051 to 0.091, where such a rise in microsegregation at these higher cooling rates result in negatively impacting mechanical properties, particularly hot ductility. Also it was reported, due to the slow diffusion rate of Mn, it is difficult to eliminate through subsequent heat treatments, resulting in microstructural inhomogeneity [7]. Furthermore, some studies have reported a non-linear trend of microsegregation levels of Mn first increasing to a peak CR 5.87℃/s (with a segregation ratio of ~1.17) and then decreasing at the highest cooling rates of 10.28℃/s (with a segregation ratio of ~1.07), where the faster cooling reduces the time for back diffusion, leading to increased segregation, the associated refinement in microstructure (smaller SDAS, and while SDAS wasn't reported, the average grain size was reported instead from around 120.17μm to 88.63μm) can also reduce the diffusion distances and therefore this can mitigate segregation at higher CR [8]. Through this work, DP800 steel grade will be investigated and the link between cooling rate, SDAS and microsegregation (particularly Mn) will be explored.

2. EXPERIMENTAL METHODS AND MATERIAL CHARACTERISATION

Compositions were cast using a Consarc Vacuum Induction Melting (VIM) furnace into one 15kg wedge mould ingot. The as-cast material was sectioned along different positions on the wedge to give a range of cooling rates for the steel samples (**Figure 1**). Due to the ingot geometry, the as-cast microstructure was martensitic, thus segregation analysis was carried out on as-cast samples. These were polished to a final 0.05μm using a non-crystallised colloidal silica solution. Scanning electron microscopy (SEM) using a JEOL JSM-7800F system equipped with Energy Dispersive X-ray Spectroscopy (EDS), to characterise the microstructure. A grid-based EDS mapping approach was developed to analyse microsegregation across dendritic structures. Each mapped region consisted of 350-450 measurement points, with a x60 magnification and constant working distance of 10mm. The grid spacing was derived from the minimum SDAS (~ 40μm), using either 1.5x SDAS or SDAS/1.5 of this value to ensure sufficient spatial resolution relative to the dendritic features whilst maintaining the minimum of 350 grid points per sample.

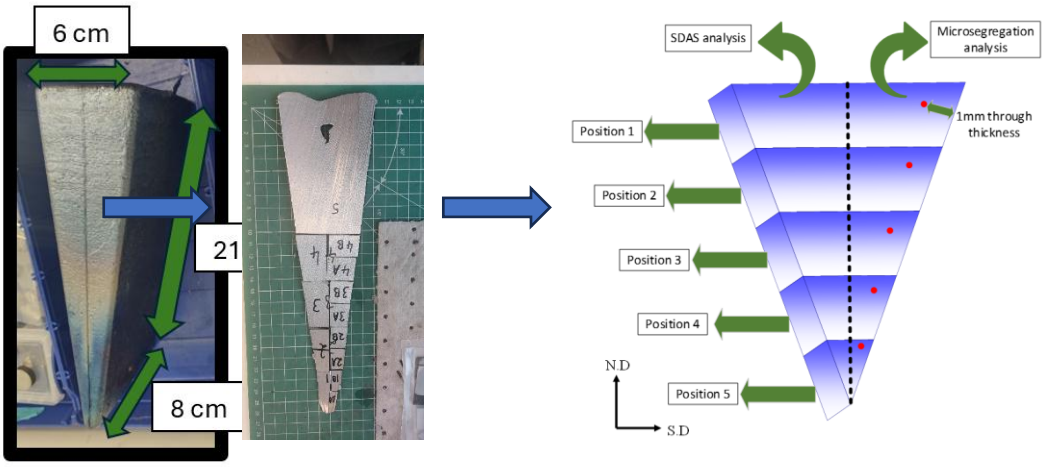

Figure 1 As-cast ingot from the wedge mould and schematic of where points taken for micro segregation analysis

In order to assess the SDAS then the samples were normalised to achieve a ferrite pearlite structure, making the dendritic structure much clearer. To achieve this heat treatment was carried out at 950℃ and held for 10 mins before being furnace air cooled to room temperature before polishing and etching with 2% Nital solution.

A Keyence VHX-7000 microscope was used to examine the dendritic structure to measure an array of secondary dendrite arm spacings at each 1mm increment through thickness. For each region, a minimum of one hundred dendrite arm spacings were measured, ensuring statistical significance, and reducing measurement variability. The compositions used in this study are detailed in **Table 1** which were measured using Optical Emission Spectroscopy (OES). A solidification heat transfer model was developed using COMSOL Multiphysics to simulate cooling rates for a DP800 steel ingot sample. The COMSOL simulation incorporated the measured SDAS values to validate the predicted cooling rates and then these cooling rates were independently verified using the CR-SDAS relationship [9]. Hence these CR were utilised in the COMSOL model to simulate CR at different positions along the wedge mould. The use of this particular SDAS-CR equation is due to the similar composition of steel analysed and hence similar SDAS and CR properties that are associated with it going hand in hand. The CR-SDAS relationship for this composition used is:

$$SDAS = 84CR^{-0.45} \quad (1)$$

Table 1 Compositions of steel grades used in this study (wt%)

DP steel grade	C	Mn	Si	S	P	Cr	Al	Nb	Fe
DP - Wedge	0.135	2.27	0.265	0.003	0.005	0.535	0.008	0.026	Bal.

3. RESULTS AND DISCUSSION

3.1 Microstructures and SDAS

The typical heat-treated dendritic microstructures for the DP wedge mould is shown in **Figure 2**. Here the microstructure is of only ferrite and pearlite phases. The measured SDAS is also shown in **Figure 2** with the solidification cooling rates shows that over the slower cooling rates ~0.68℃/s to 1.27℃/s, the SDAS values ranged from 104.01µm to 69.76µm and showed a sharp initial decrease in the arm spacing. At the higher cooling rates ~3.45℃/s to 5.8℃/s the decrease in the SDAS was less pronounced at 45.36µm to 40.02µm, which is widely reported in literature that the SDAS sensitivity is significantly less at higher cooling rates [10].

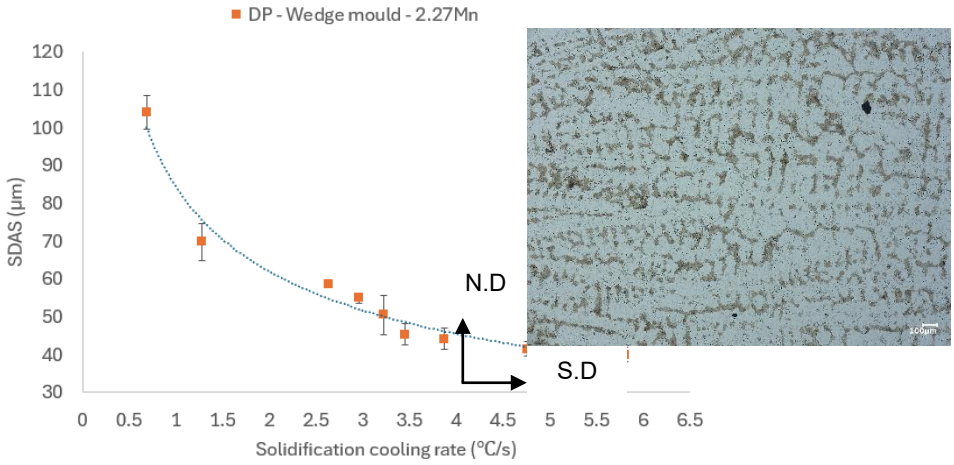

Figure 2 SDAS for 2.27Mn wedge mould for a range of solidification cooling rates and heat-treated ferrite-pearlite microstructure

3.2 Microsegregation Microstructures and SDAS

The as-cast samples for the DP wedge mould was analysed for the level of microsegregation of Mn, **Figure 3** illustrates how the segregation ratio develops over the solidification cooling rate. To quantify Mn segregation, a weighted ranking number system was utilised to investigate the segregation ratio (SR) of Mn. This involves ranking the Mn concentration measurements from lowest to highest and calculating a SR of the minimum to maximum values in each region. However maximum concentrations of Mn may include MnS (inclusion hit regions) and therefore a 95th and 5th values were utilised instead of maxima and minimum values. This was the Mn content over the average bulk Mn composition, which enabled to exclude the MnS regions. The segregation ratio was defined as:

$$SR = \frac{95th\ percentile\ value}{5th\ percentile\ value} \quad (2)$$

From **Figure 3** the DP wedge shows a complicated behavioural profile, where the SR trends observed here are consistent with previous studies; where first Li, Y. et al. reported Mn segregation intensity initially increased with CR from segregation ratio of ~1.1 to ~1.3 but then slightly decreased at the highest of cooling rates to ~1.25, with a confocal scanning laser electron microscope was utilised to set the solidification cooling rates of 6℃/min, 50℃/min and 100℃/min. Huan, et. al. also reported microsegregation levels to increase initially with CR, reaching a peak at the highest CR (the CR here were calculated by thermocouples connected to a temperature recorder, and hence average CR of different diameter ingots was calculated) [8, 11]. The DP wedge in this study can be broken down into three sections;

1. A decrease in SR at lower cooling rates (from around 0.6℃/s to 2.6℃/s) due to SDAS refinement.

2. An increase in SR at mid-range CRs (from around 2.6℃/s to 4.75℃/s) likely due to reduced back diffusion time.

3. A plateau or slight decrease in SR at the highest of CRs (from around 4.75℃/s to 5.8℃/s), possible due to the post solidification CR not changing despite increasing through solidification CR from the COMSOL model. In ideal conditions, the faster solidification CR might also result in a faster post solidification CR, however due to the geometry of the wedge mould the post solidification CR remains unchanged across the higher CR range (from around 4.75℃/s to 5.8℃/s), providing similar conditions for solute back diffusion. As back diffusion is dependent on temperature and time, this flattening of post solidification profile could explain why further increases in solidification CR does not lead to a continued increase in SR.

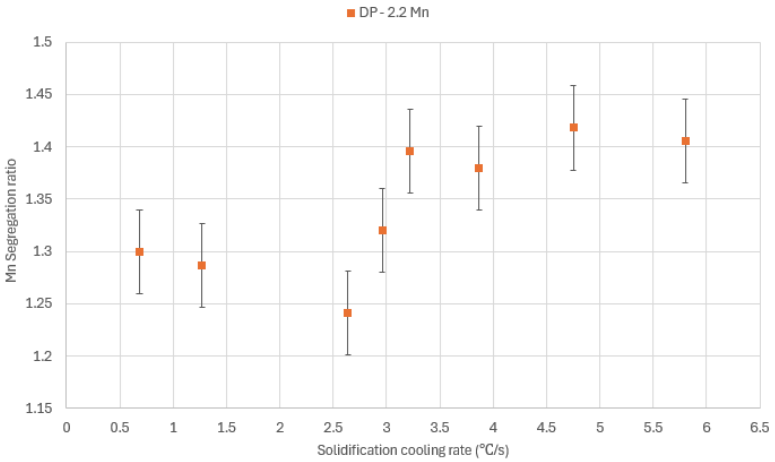

Figure 3 Microsegregation for 2.27Mn wedge mould across a range of solidification cooling rates

3.3 Predictive Thermo-calc analysis

As the DP wedge mould showed a complex SR profile over a range of solidification CR a Thermo-Calc DICTRA simulation was deployed to see the predictive relationship. The time-temperature profile from COMSOL was used in Thermo-Calc for the post solidification behaviour of the DP wedge mould. Specifically, the cooling curve from the solidus temperature down to approximately 1000 ℃ allowing for the prediction of post-solidification cooling (during solidification the predicted cooling rates were utilised for the analysis). **Figure 4** shows a similar trend was observed with Thermo-Calc DICTRA predictions for Mn SR.

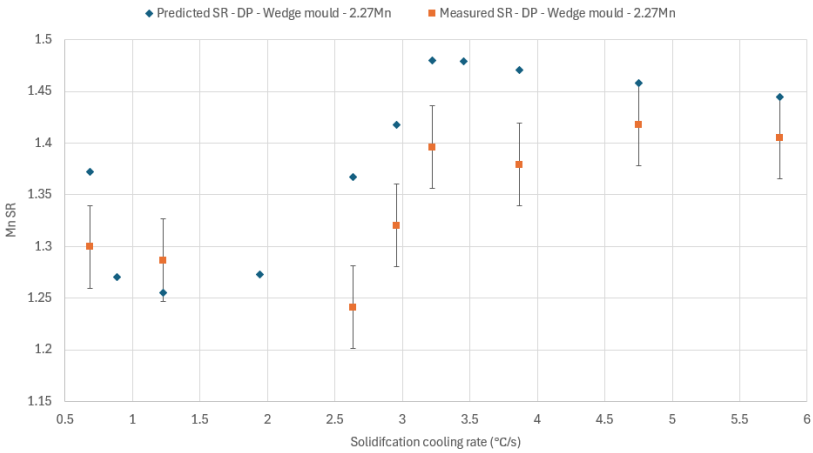

Figure 4 Predicted and measured Mn SR for 2.27Mn wedge mould

This predictable trend in segregation ratio at various cooling rates, whilst initially appears unintuitive and complex, shows good agreement with Thermocalc. To understand this complex curve then first the two competing factors need to be assess. These are:

1. The diffusion distance i.e. SDAS
2. The diffusion time i.e. cooling rate

Firstly, to understand what is happening here, the cooling profiles for specific locations are shown in **Figure 5**. As observed from **Figure 5**, the higher solidification rate e.g., at 5.8℃/s experienced a rapid drop in temperature, reaching 1000℃ in under 70 seconds, whereas the slower cooling rate of 1.94℃/s retained heat for significantly longer and did not reach 1000℃ even after 300 seconds. This reflects the efficiency of heat extraction under faster cooling conditions, where the heat is lost to surroundings due to contact with the colder mold walls and better conduction, resulting in a steeper drop in temperature over time. At the 1.94℃/s the heat extraction is relatively poor, because this region is closer to the centre of the ingot, where the thermal gradient is lower due to the increased distance from the mould wall, thus retaining the heat for longer and solidifying more slowly.

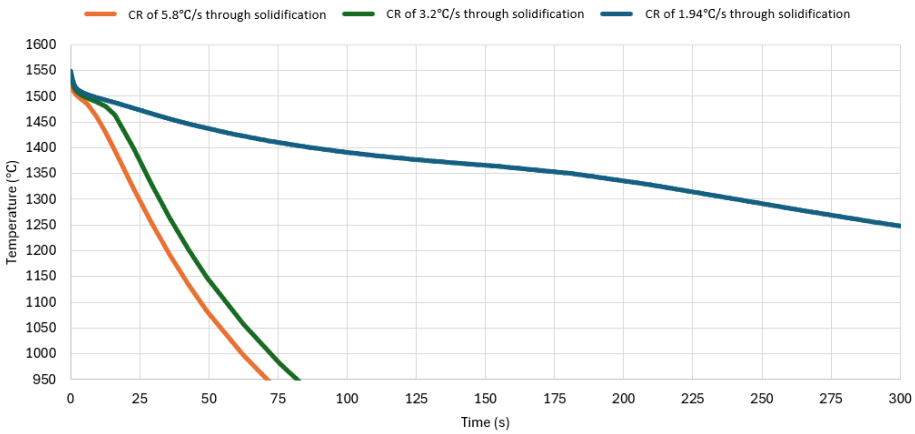

Figure 5 Temperature-time curves for different points along the 2.27Mn wedge mould

To investigate the complex behaviour further, thermal energy was used and calculated as the integral of the temperature-time profile curve. This approach helps in evaluating whether differences in post solidification cooling can explain the SR profile. **Figure 6** shows the calculated thermal energy profiles of the 2.27Mn wedge mould. The 2.27Mn wedge mould shows a non-linear trend, where a decrease in thermal energy can be seen with CR initially (around 0.68℃/s to 2℃/s) and thereafter the thermal energy dropping even more rapidly (around 2℃/s to 3℃/s) then the thermal energy plateaus in the region around (600℃s to 700℃s in thousands) for CRs above 3℃/s. This plateau suggests that even at the highest solidification rates that due to a combination of latent heat, surround liquid with lower thermal conductivity and mould geometry, the post solidification cooling rate is much less sensitive to the position within the wedge mould, and as such solidification rate and post solidification cooling rate are not dependent variables. As such this plateau in thermal energy at solidification rates greater than 3 °C/s provides a constant level of back diffusion, and indicates a convergence in post solidification cooling which helps explain the observed Mn SR at higher CRs (**Figure 4**).

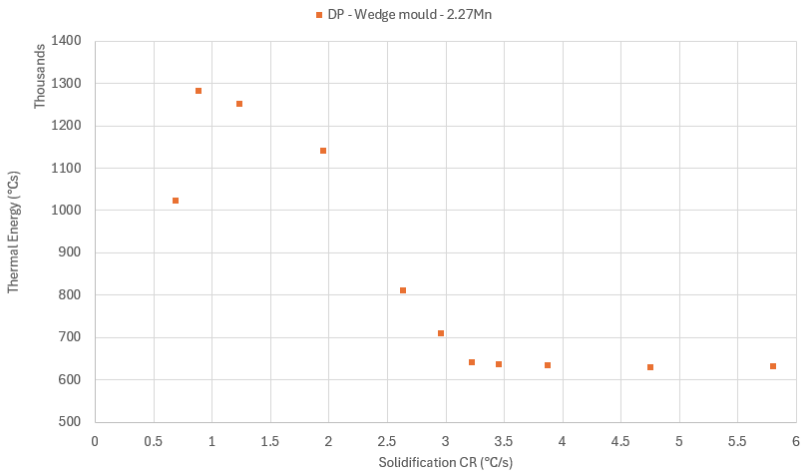

Figure 6 Thermal energy change with respective solidification cooling rates for 2.27Mn wedge mould

SR is proportional to the SDAS but inversely proportional to thermal energy and therefore the metric of SDAS/Thermal energy has been used to simplify the comparison. **Figure 7** compares the predicted Mn SR with the SDAS/Thermal energy ratio across the range of solidification CRs for the 2.27Mn wedge mould. This comparison was made to assess whether SDAS and thermal energy can provide insight into the trend of microsegregation. By plotting SDAS/thermal energy against predicted Mn SR the aim was to evaluate if

SDAS/thermal energy could explain the observed plateau in SR at higher CRs. The results show a clear alignment, as SDAS/thermal energy drops (particularly above 3℃/s), the predicted SR reaches a plateau.

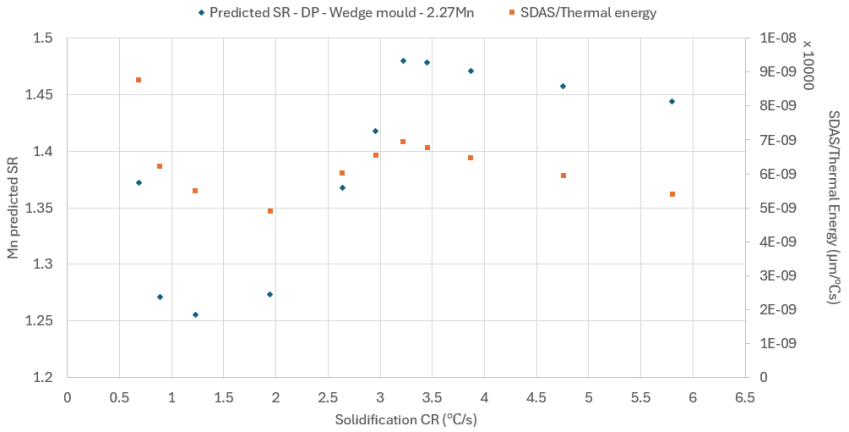

Figure 7 SDAS/Thermal energy ratio with the predicted 2.27Mn SR for the wedge mould

3.4 Consequence of Casting Technologies

Measured microsegregation results and predicted microsegregation levels showed good agreement. Therefore, utilising the predictive features from ThermoCalc and known literature for solidification and post solidification cooling rates, a predicted microsegregation analysis can be conducted for casting technologies. **Figure 8a** shows the calculated temperature-time profiles for the conventional continuous caster (CCC), thin slab caster and strip caster (considering the through solidification and post solidification rates for the different technologies) and **Figure 8b** showing the predicted Mn segregation ratios for the respective casting technologies [2, 4, 5, 12, 13].

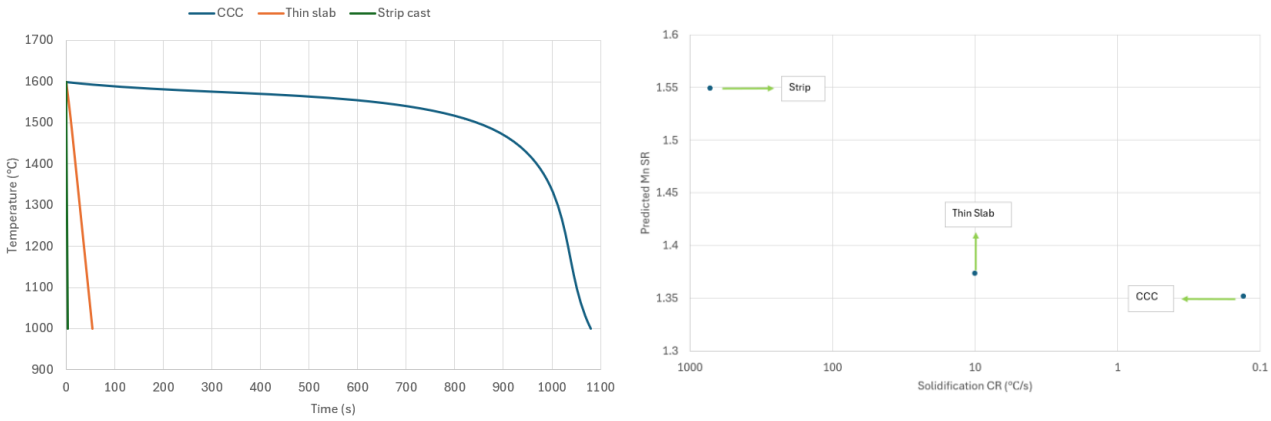

Figure 8 a) temperature-time profile of CCC, thin slab and strip casters and b) predicted Mn SR for CCC, thin slab and strip casters

As seen from **Figure 8** the Mn SR increases as the CR increases. Strip casting with the highest CR exhibits the greatest Mn SR of about 1.55 while CCC, with the lowest CR shows the least segregation at 1.35. this trend is expected as the slower cooling seen in CCC provides more time for back diffusion and reducing segregation as a result. Conversely at higher cooling seen in strip casting, here there is limited time for back diffusion to occur and an increase in SR.

4. CONCLUSION

The findings in this study were presented for a DP wedge where the Mn SR and SDAS behaviour in steels across a range of solidification cooling rates were evaluated. As expected, a clear inverse relationship between CR and SDAS was observed. Interestingly, Mn SR decreased initially with increasing CR but showed complex behaviour in wider CR ranges. ThermoCalc-DICTRA simulations confirmed the experimental trends for measured SR, validating the impact of post-solidification profiles on segregation. The SDAS/thermal energy ratio correlated well with predicted Mn SR. Additionally, the measured experimental SR coupled with predictive SR also correlated well for the SR seen in the different casting technologies.

REFERENCES

[1] LUITEN, E.E.M., BLOK, K. Stimulating R&D of industrial energy-efficient technology; the effect of government intervention on the development of strip casting technology. *Energy Policy*. 2003, vol. 31, pp. 1339-1356.

[2] WANG, W., ZHU, M., CAI, Z., LUO, S., JI, C. Micro-Segregation Behavior of Solute Elements in the Mushy Zone of Continuous Casting Wide-Thick Slab. *Steel Research International*. 2012, vol. 83, pp. 1152-1162.

[3] SLATER, C., KOSTRYZHEV, A., MARENYCH, O., DAVIS, C. Implications of Accelerated Solidification Rates Seen in Belt Casting on Precipitation in Nb Bearing Steels. *Steel Research International*. 2018, vol. 89.

[4] XU, P., YIN, F., NAGAI, K. Solidification cooling rate and as-cast textures of low-carbon steel strips. *Materials Science and Engineering A*. 2006, vol. 441, pp. 157-166.

[5] DAAMEN, M., SCHWEINICHEN, P., RICHTER, S., SENK, D., HIRT, G. Strip casting and ingot casting: comparison of different cooling conditions regarding the as-cast quality. IN: *8th European Continuous Casting Conference (ECCC-2014)*. pp. 1271-1281.

[6] ZHANG, W., LIU, L., ZHAO, X., HUANG, T., YU, Z., QU, M., FU, H. Effect of cooling rates on dendrite spacings of directionally solidified DZ125 alloy under high thermal gradient. *Rare Metals*. 2009, vol. 28, pp. 633-638.

[7] ZHAO, L., SONG, Y., ZHAI, G., LIU, H., CHEN, X., ZHAI, Q. Effect of cooling rate on solidification microstructure, microsegregation, and nanoprecipitates in medium carbon CrMo cast steel. *Journal of Materials Research and Technology*. 2024, vol. 31, pp. 635-648.

[8] HUANG, S., LI, G., ZHANG, Z., TAN, Q., ZHU, G. Effect of Cooling Rate on the Grain Morphology and Element Segregation Behavior of Fe-Mn-Al-C Low-Density Steel during Solidification. *Processes*. 2022, vol. 10, pp. 1101.

[9] VOLKOVA, O., HELLER, H-P., JANKE, D. Microstructure and Cleanliness of Rapidly Solidified Steels. *ISIJ International*. 2003, vol. 43, pp. 1724-1732.

[10] LIANG, C., SONG, G., LIANG, L., WANG, W., ZENG, J. Effect of Solidification Cooling Rates and Subsequent Homogenization Treatment on Mn–Cr–Mo Element Segregation in Oil Casing Steels. *Metals and Materials International*. 2024, vol. 30, pp. 2269-2281.

[11] LI, Y., ZOU, D., CHEN, W., ZHANG, Y., ZHANG, W., XU, F. Effect of Cooling Rate on Solidification and Segregation Characteristics of 904L Super Austenitic Stainless Steel. *Metals and Materials International*. 2022, vol. 28, pp. 1907-1918.

[12] LAN, P., LIU, H., ZHANG, J., LU, Y., ZHANG, L. Austenite grain growth in tailored cooling rate experiment designed by numerical simulation for peritectic steel. *Journal of Materials Research and Technology*. 2024, vol. 33, pp. 3405-3417.

[13] XIONG, Z.P., KOSTRYZHEV, A.G., STANFORD, N.E., PERELOMA, E.V. Microstructures and mechanical properties of dual phase steel produced by laboratory simulated strip casting. *Materials & Design*. 2015, vol. 88, pp. 537-549.